Functional & Mechanistic Neurotoxic Profiling Using Human iPSC-Derived Neural Spheroid 3D Cultures

Oksana Sirenko[1], Frederick Parham[3], Neha Sodhi[2], Kristen Ryan[3], Mamta Behl[3], Grischa Chandy[1], Matthew Hammer[1], Carole Crittenden[1], Sarah Vargas-Hurlston[1], Kendra Prum[2], Fabian Zanella[2], Cassiano Carromeu[2]

[1]Molecular Devices LLC, San Jose, California, US; [2]StemoniX Inc., Maple Grove, MN, US, [3]Division of the NTP, US

StemoniX®

INTRODUCTION

Neurological disorders affect millions of people worldwide and appear to be on the rise. While the reason for this increase remains unknown, environmental factors are a suspected contributor. Hence, there is an urgent need to develop more complex, biologically relevant and predictive in vitro assays to screen potentially neurotoxic compounds. Here, we employed a human induced pluripotent stem cell (iPSC)-based 3D neural platform composed of mature cortical neurons and astrocytes. This advanced neural platform was optimized for high throughput screening in 384-well plates and displays a highly consistent, functional performance across different wells and plates. With this model, we explored the neurotoxic profile of a library of 87 unique compounds that included pharmaceutical drugs, pesticides, flame retardants, and other chemicals.

Results: After removing compounds that were not expected to show results in the microBrain 3D platform, 61% of tested compounds exhibited effects in the assay. Our results show that the iPSC-derived 3D neural spheroid assay platform is a promising biologically-relevant tool to assess the neurotoxic potential of drugs and environmental toxicants.

1 iPSC-Derived microBrain® 3D

StemoniX® microBrain® 3D Assay Ready Platform is a high throughput compatible platform that more closely resembles the tissue development and constitution of native human brain tissue. In this platform, human iPSC-derived neuronal spheroids, approx. 600 mm diameter, are composed of a physiologically relevant co-culture of functionally active cortical glutamatergic and GABAergic neurons (identified by MAP2; green) and astrocytes (identified by GFAP; red). This balanced cellular mix allows the development of a neural network enriched in synapses, creating highly functional neuronal circuitry. The neuronal cells in the microBrain 3D spheroids are physiologically active, with spontaneous synchronized, readily detectable calcium oscillations.

StemoniX microBrain 3D spheroids: brightfield image and immunostaining

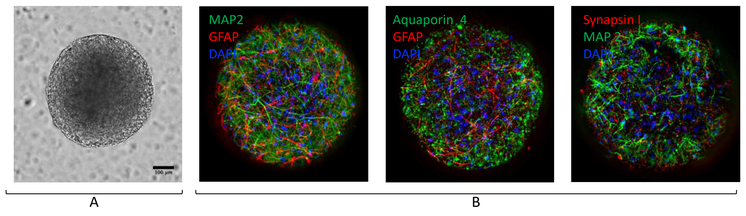

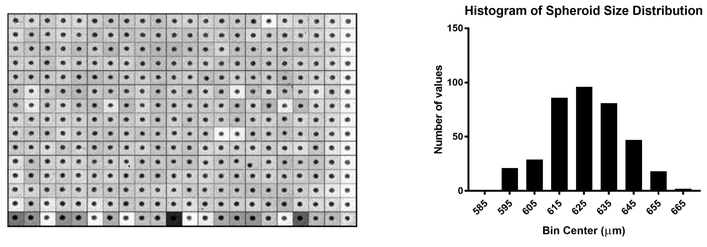

Figure 1. A. Human iPSC-derived neural spheroids, approximately 600 µm diameter, imaged with ImageXpress Micro Confocal Imaging System (IMX-C), 20x magnification, transmitted light. B. Fluorescent images were taken after staining cells with marker-specific antibodies as described in Materials and Methods. Images were taken using 20x objective in confocal mode. Spheroids are composed of a co-culture of active cortical neurons (identified by MAP2; green) and astrocytes (identified by GFAP; red)

METHODS

Instruments

We used fast kinetic fluorescence imaging on the FLIPR® Tetra System to measure the $Ca2^{2+}$ oscillations of neural spheroids as monitored by changes in intracellular Ca^{2+} levels with Calcium 6 dye (Molecular Devices). Cell imaging analysis was done using the ImageXpress® Micro XL Confocal Imaging System (IXM-C) in combination with the MetaXpress® 6.5 High-Content Imaging Software (MX 6.5).

3D neural cultures

microBrain® 3D Assay Ready 384-Well plates were obtained from StemoniX, Inc. Plates were shipped pre-plated under ambient conditions. Each well contained a single, uniformly sized human iPSC-derived cortical neural spheroid matured 8-9 weeks. The human spheroids were exposed to compounds for 24 hours, or as indicated in the figures.

Calcium Flux Assay

The intracellular Ca^{2+} oscillations were assessed using the Calcium 6 dye (Molecular Devices); spheroids were loaded with dye for 2 hours before measurements.

Cell Staining

To assess phenotypic changes, cells were stained live using a mixture of three dyes: the viability dye Calcein AM (1 mM), the mitochondria potential dye MitoTracker Orange (0.2 mM), and the Hoechst nuclear dye (2 mM). For assessment of neuro-specific markers cells were fixed with 4% formaldehyde (Sigma) and stained with anti-TuJ-1 and anti GFAP antibodies (Becton Dickinson).

RESULTS

2 Calcium Oscillations Evaluated by FLIPR

microBrain 3D spheroids generate spontaneous, synchronized calcium oscillations. We used the FLIPR® Tetra System to measure the patterns and frequencies of the Ca^{2+} oscillations of neural spheroids as monitored by changes in intracellular Ca^{2+} levels with Calcium 6 dye. A set of known neuromodulators was tested, including agonists and antagonists of NMDA, GABA and AMPA receptors, kainic acid, analgesic and anti-epileptic drugs.

3D neural spheroid stained with Calcium 6 dye:

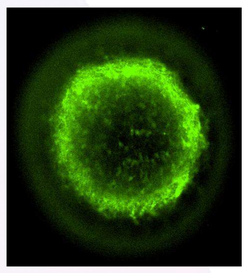

Calcium oscillation traces recorded by FLIPR instrument:

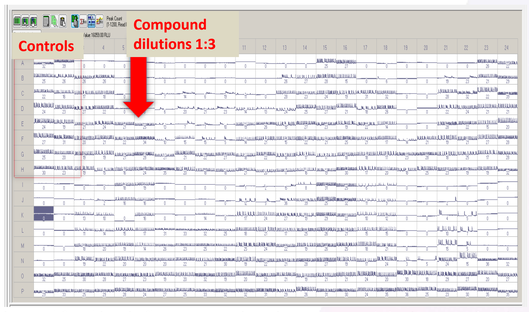

Figure 2. Using high-content imaging and fast kinetic fluorescence imaging, we tested the impact of various compounds on Ca^{2+} oscillations. Left: Confocal image of 3D spheroid (10x) stained with Calcium 6 dye (green). Right: High-throughput recording and analysis of the entire 384-well plate simultaneously using the FLIPR system and PeakPro software. Oscillation traces were recorded by FLIPR system for 10min. Concentration-dependent changes in the patterns were observed and characterized using PeakPro software.

3 Analysis of Kinetic Patterns: Measurements and Variability

Advanced analysis methods were implemented to provide multi-parametric characterization of the Ca^{2+} oscillation patterns. This phenotypic assay allows for the characterization of read-outs such as peak count, amplitude, width, rise and decay times. The effects of modulators of neuronal activity were evaluated by measuring changes in the read-out values. The precision and variability of the measurements was evaluated for 24 control wells for different time-points after compound addition.

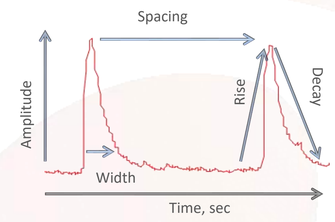

Measurements:
1. Peak count (per 10 min of recording)
2. Average peak amplitude
3. Average spacing between peaks
4. Average peak width (10% amplitude)
5. Average peak rise time
6. Average peak decay time

Figure 3. Descriptors for the phenotypic changes measured. The intracellular Ca^{2+} oscillations were assessed using Calcium 6 Dye.

4 Assessment of Spheroid Morphology and Viability by High Content Imaging

Confocal imaging and 3D image analysis methods were used to characterize compound effects on the cell viability of 3D neural spheroids. To evaluate cytotoxicity, cells were treated with various compounds for 24h, and then stained with Hoechst nuclear stain, Calcein AM, and MitoTracker Orange dye. Images were acquired using the IXM-C System confocal option and 3D imaging. Projection images were then analyzed using the Custom Module Editor and Cell Scoring algorithms.

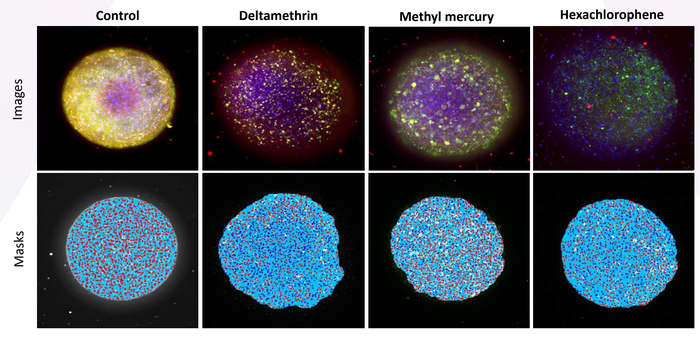

Figure 5. Spheroids were treated with 30 µM of compounds for 24h, then stained with Hoechst 33342, Calcein AM, and MitoTracker Orange CMTMRos for 2 hours (2 µM, 1 µM, and 0.5 µM). Spheroids were imaged using Z-stack of confocal images. Maximum projection images were analyzed using custom module editor for detection of spheroid size and shape, and positive and negative cell count in the spheroid. The image show nuclei (blue), Calcein AM stain (green), and mitochondria (orange). The mask showing spheroids in blue, nuclei of Calcein AM positive cells in red, negative cells in blue.

RESULTS

5 Evaluation of Neurotoxicity Effects Using Selected Set of Neurotoxic Compounds

The assay show promise for the high throughput assessment of neurotoxicity effects of chemicals in vitro which would help to evaluate and prioritize different substances for further testing. We have tested 87 unique compounds that represent different classes of toxic chemicals, including flame retardants, pesticides, poly-aromatic hydrocarbons, and demonstrated sensitivity of the assay to the number of known neurotoxicants. Overall, the functional assay identified significantly more neurotoxins than either of the cell viability assays tested.

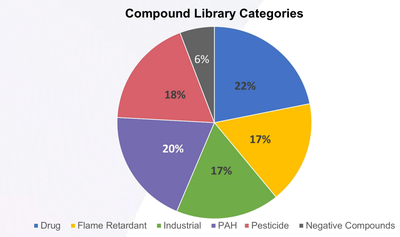

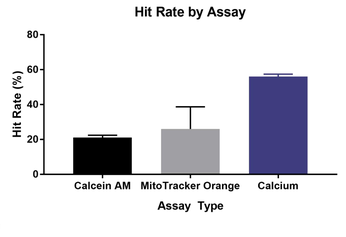

Figure 4. Left: Breakdown of compounds by type. Right: Graph of hit rate by assay. Calcium assay values listed are using the peak count parameter.

6 Assessment of Compound Action on microBrain® 3D Platform

The screening results were further analyzed by subclass, with pesticides, flame retardants, drugs and industrial chemicals showing significantly greater sensitivity to calcium oscillations than cell viability. Also of note, the library contains several compounds, particularly drug compounds, that were not expected to show results in microBrain 3D, as shown in the table below. For example, 5-FU, colchicine, and hydroxyurea are all involved in cell proliferation. As microBrain 3D is terminally differentiated, a response was not expected. Two other compounds were removed due as a response was not expected in this model. Sensitivity of the model accounting for appropriate target cell population, age, and mechanism of action rose to 61%.

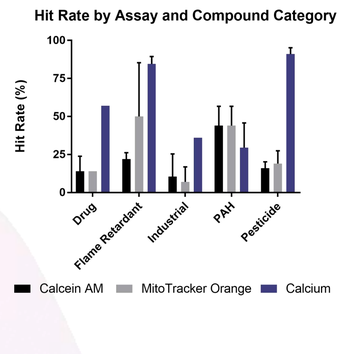

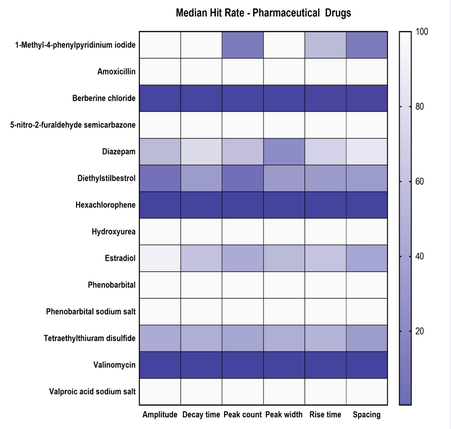

CONCLUSIONS

We developed the methods and demonstrated feasibility of the iPSC-derived StemoniX microBrain® 3D Assay Ready neural cultures for evaluation of compound effects. The assay can be used for testing compound effects and screening for neurotoxic chemicals

The significant advantage of microBrain 3D for drug screening and toxicology studies is the highly homogeneous calcium signal achieved across the plate and between different plates and batches. We have shown through this work that the platform is more sensitive than cell viability assays for the toxins presented in this library. The microBrain 3D platform is particularly sensitive towards compounds in the flame retardant and pesticide classes of compounds, and is a great screening alternative to the current standards.

REFERENCES

Sirenko *et al.*, Tox. Sci. 167(1), 58-76 (2019)
Khademhisseini *et al.* Proc. Natl. Acad. Sci. USA, 103 2480-2487 (2006)
Kunz-Schughart *et al.*, J. Biomol. Screen. 9, 273–285 (2004)
Langer and Tirrell, Nature 428, 487–492 (2004)
Rathod *et al.* J. Chem. Neuroanat. 95,81-88 (2019)
Horman *et al.* Future Med. Chem. 7(4), 513–525 (2015)
Frank *et al.*, Tox. Sci. 160(1), 121-135 (2017)
Vargesson. Birth Defects Res. C: Embryo Today. 105, 140–156 (2015)
Quevedo *et al.* Biobide.com